• RESEARCH PAPER •

Effects of external stimuli on the pacemaker function of the sinoatrial node in sodium channel gene mutations models

ZHANG JiQian[1,2†*], LI Xiang[1†], LIANG LiSi[1], HUANG ShouFang[1] & ZHANG HengGui[2]

[1]*College of Physics and Electronic Information, Anhui Normal University, Wuhu 241000, China;*
[2]*Biological Physics Group, School of Physics & Astronomy, The University of Manchester, Manchester M139PL, UK*

Loss of function and gain of function mutations of the sodium channel were investigated using an intact two-dimensional rabbit sinoatrial node (SAN) and atrial cell model. The effects of three external stimuli (acetylcholine secretion by the vagal nerve, acid-base concentration, and tissue temperature) on cardiac pacemaker function and conduction were studied. Our results show that these two groups of mutations have different effects on pacemaker function and conduction. Furthermore, we found that the negative effects of these mutations could be altered by external stimuli. The bradycardic effects of mutations were magnified by an increase in acetylcholine level. Changes in acid-base concentration and tissue temperature increased the ability of the SAN to recover its pacemaker function. The results of this study increase our understanding of sodium channel disorders, and help to advance research on the treatment of these conditions.

gene mutation, computer simulation, sodium channel, abnormal pacemaker, 2D rabbit sinoatrial node cell model

Cell physiological activity is affected by the structure and function of ion channels. Site-specific gene mutations may lead to ion channel activation or inactivation, causing functional tissue disorders or genetic diseases [1]. The study of gene mutations may provide important information to help with the prevention and treatment of malaria in the Myanmar population [2]. Mutations of the *SCN5A* gene encoding the Na^+ channel can lead to abnormalities of Na^+ channel structure and function, resulting in arrhythmias [3].

There are three types of Na^+ channel mutation: loss of function mutations (LFMs), gain of function mutations (GFMs), and non-functional mutations (NFMs). LFMs result in Na^+ current and accelerated channel inactivation. GFMs result in increased Na^+ current and delayed channel inactivation, so that the channel remains open and slows down the increase in the sodium current, thereby increasing

the duration of the action potential. LFMs may cause Brugada syndrome [4–6], sick sinus syndrome [7,8], and progressive familial heart block type I [9]. GFMs may cause long QT syndrome [10,11] and sudden infant death syndrome [12,13]. *SCN5A* gene mutations may have complex clinical manifestations termed cardiac sodium channel overlap syndromes [14]. However, there is currently no evidence that NFMs affect the function of the Na^+ channel.

Recent experimental studies have examined the effects of LFMs and GFMs at the molecular level. We previously reported that environmental changes may affect intracellular ion movement [15,16]. We wanted to evaluate whether defective Na^+ channel function resulting from gene mutations can be ameliorated, by determining whether pacemaker and conduction can be improved by external stimuli.

This study used computer simulations to study the effects of three external stimuli on pacemaker function and conducting in an intact two-dimensional (2D) rabbit sinoatrial

†Contributed equally to this work
*Corresponding author (email: zhangcdc@mail.ahnu.edu.cn)

node (SAN) and atrial cell model to evaluate Na$^+$ channel LFMs and GFMs.

1   Materials and methods

To study the ionic mechanisms of cardiac pacemaker function with the gene mutations, an anatomical model for the electrical action potentials of the SAN and atrial cells of the rabbit heart was used as follows [17,18]:

$$C_m \frac{\mathrm{d}V}{\mathrm{d}t} = -(I_0 + I_{Na} + I_{CaL} + I_{CaT} + I_{K,ACh}) = -I_{tot},$$

$$I_0 = I_{NaK} + I_{NaCa} + I_K + I_{to} + I_{st} + I_f, \tag{1}$$

where V is the membrane potential, C_m is the cell membrane capacitance (μF), I_{Na} is the tetrodotoxin-sensitive Na$^+$ current, I_{CaL} and $I_{K,ACh}$ are L-type Ca^{2+} channel currents, and I_0 is the acetylcholine (Ach) activated K$^+$ channel current, details of the equations for the currents and the parameters of the model have been published elsewhere [17,18].

Cardiac pacemaker function is a complex collective behavior. To investigate the effects of external stimuli on this function, we used a model based on rabbit heart atrial muscle cells of the crista terminalis and the intercaval region, and central and peripheral SAN cells. The SAN and atrial cell model units were used to construct a 375×45-node network. Each node represented a cell, and each cell satisfied the parameters of eq. (1). The intact 2D anatomical model satisfied the following equation [18]:

$$C_m(i,j)\frac{\partial V(i,j)}{\partial t} = -I_{tot} + \nabla \cdot [D(i,j)\nabla V(i,j)], \tag{2}$$

where (i, j) is the spatial location, $D(i, j)$ is the diffusion coefficient that characterizes electronic spread of the voltage via gap junctions, and ∇ is the spatial gradient operator in a cell.

This study investigated the effects of three external stimuli on SAN pacemaker function in Na$^+$ channel LFM and GFM models. In our simulations, the time step was set to 0.005 ms, and the space step was set to 0.04 mm. The finite difference method was used. Cells were spatially distributed on a recording line from the center of the SAN to the periphery of the SAN and the atrium, and the action potentials of cells on this line were recorded. The cycle length (CL) was calculated from one SAN cell on this recording line.

2   Results and discussion

We studied the effects of Na$^+$ channel LFMs and GFMs on SAN pacemaker function. These groups of gene mutations may cause abnormal Na$^+$ channel function, and some mutations are associated with arrhythmias. The corresponding I_{Na} is modeled by the following equation:

$$I_{Na} = (kg_{Na})m^3h[Na]_0^+ \frac{VF^2}{RT}\frac{\mathrm{e}^{(V-E_{Na})F/RT}-1}{\mathrm{e}^{VF/RT}-1}, \tag{3}$$

where g_{Na} is the Na$^+$ channel conductance, and m and h are the activation and inactivation variables. For this mutation model, the effect of the mutation is denoted by the parameter k. If $k<1$, the Na$^+$ current is decreased, indicating LFM; and if $k>1$, the Na$^+$ current is increased, indicating GFM [19]. Details of eqs. (1)–(3) have been published elsewhere [17–19].

The effects of Na$^+$ channel LFMs and GFMs on pacemaker function in our model are shown in Figure 1. Com-
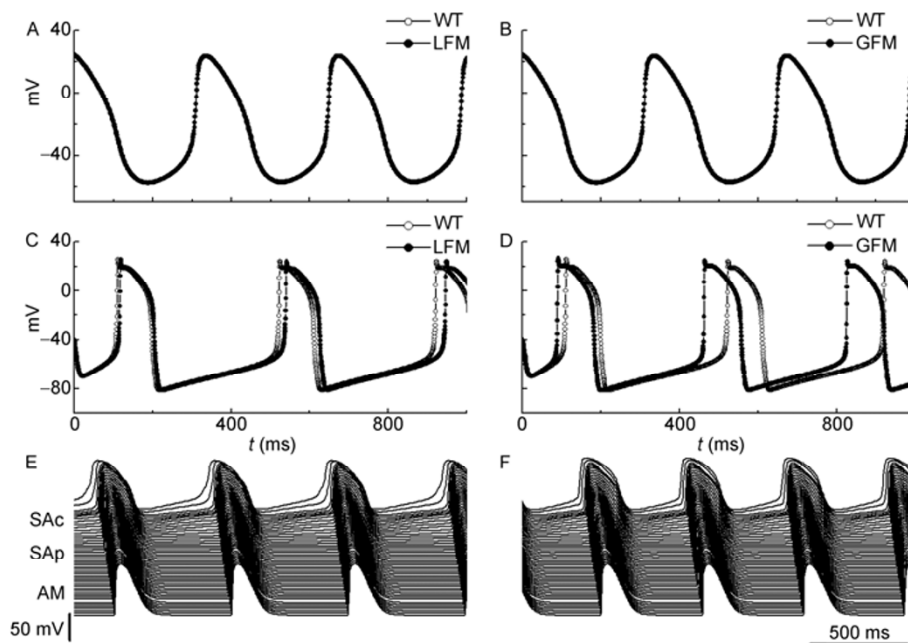

Figure 1   Effects of mutations on SAN pacemaker function. Left panel, LFM model; right panel, GFM model. A and B, Effects of mutations on central SAN (SAc) cells. C and D, Peripheral SAN (SAp) cells. E and F, Atrial muscle (AM) cells.

pared with normal pacing rates in a wild-type model (normal *CL*=274.15 ms), the LFM model had a lower pacing rate in peripheral SAN cells (Figure 1C) but not in central SAN cells (Figure 1A). Similarly, the GFM model had a higher pacing rate in peripheral SAN cells (Figure 1D) but not in the central SAN cells (Figure 1B) [19,20]. In the 2D tissue model without ACh, the LFM model had a lower pacing rate, which could lead to sinus bradycardia and sinus arrest (Figure 1E; *k*=0.6, *CL*=297.9 ms), and the GFM model had a higher pacing rate, which could lead to tachycardia and atrial fibrillation (Figure 1F; *k*=1.4, *CL*=257.5 ms).

2.1 External stimulation of the vagal nerve

To study the effects of the neurotransmitter ACh on pacemaker function in the Na^+ channel LFM and GFM models, we chose conductance of ACh-dependent currents (i.e., $I_{K,ACh}$ and $I_{Ca,L}$) and [ACh] as the controllable parameters [17]. The dynamics of these currents are described by the following equations:

$$I_{K,ACh} = g_{K,ACh} \left(\frac{[K^+]_e}{10 + [K^+]_e} \right)$$

$$\times \left(\frac{V_m - E_K}{1 + \exp[(V_m - E_K - 140)F / 2.5RT]} \right),$$

$$I_{Ca,L} = g_{Ca,L} \left[f_L d_L + \frac{0.006}{1 + e^{-(V+14.1)/6}} \right] (V - E_{CaL})(1-b),$$

$$g_{K,ACh} = g_{K,ACh,max} jk \frac{[ACh]^{n_{K,ACh}}}{K_{0.5,K,ACh}^{n_{K,ACh}} + [ACh]^{n_{K,ACh}}}, \qquad (4)$$

where $g_{K,ACh}$ and $g_{Ca,L}$ are channel conductance values, $g_{K,ACh,max}$ is the maximum value of $g_{K,ACh}$, j and k are inactivation variables, and [ACh] is the concentration of ACh. The general descriptions and details of the other currents in the equations shown in (4) have been published elsewhere [17–19].

The spatiotemporal evolution of action potentials was recoded for cells from SAN to the atrium on the recording line (Figure 2). When [ACh]=0.0, the action potential was initiated in the center of the SAN and then propagated to the periphery of the SAN and atrium (Figure 2A). When [ACh] was increased to $1.5×10^{-8}$ mol L^{-1}, the CL increased in the wild-type model from 274.4 to 321.5 ms (Figure 2B), indicating the negative effect of ACh. In the mutation, the abnormal pacemaker function was amplified and exhibited different characteristics. In the LFM model with *k*=0.6, the pacemaker rate decreased and the *CL* increased to 363 ms (Figure 2C). If [ACh] was further increased to $5.0×10^{-8}$ mol L^{-1}, the SAN pacing rate decreased further or even stopped completely (data not shown). In the GFM model with *k*=1.4, the CL increased to 293 ms (Figure 2D). The results of the LFM simulation are consistent with the clinical characteristics of this condition. As the ACh concentration in the SAN is higher during sleep at night than during the day, the heart
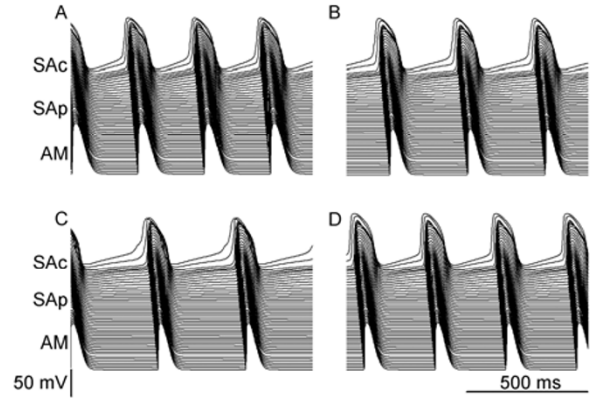

Figure 2 Effects of [ACh] on SAN pacemaker function. A, Normal tissue without ACh, *CL*=274.15 ms. For B–D, [ACh]=$1.5×10^{-8}$ mol L^{-1}. B, Normal tissue, *CL*=321.45 ms. C, LFM model (*k*=0.6), *CL*=363 ms. D, GFM model (*k*=1.4), *CL*=293 ms.

rate may decreased or may even stop causing sudden death, in patients with relevant heart conditions [6,21].

2.2 Adjustment of the acid-base concentration by drug treatment

Recent experimental results show that the Ca^{2+} channel current $I_{Ca,T}$ is sensitive to acid-base concentration [22]. A highly acidic concentration may inhibit the transport of Ca^{2+} and the activities of some enzymes in myocardial cells, block the effects of adrenalin on the heart, and lead to decreased myocardial contractility and a flaccid myocardium. To reduce the negative effects of the mutations and improve pacemaker function, we increased the pH value of the tissue by adjusting α, the conductivity parameter of the current $I_{Ca,T}$, using the following equation:

$$I_{Ca,T} = \alpha \cdot g_{Ca,T} \cdot d_T \cdot f_T \cdot (V - E_{Ca,T}). \qquad (5)$$

We fixed [ACh]=$1.5×10^{-8}$ mol L^{-1} and adjusted the conductivity parameter α. The effects of acid-base concentration on pacemaker function in the LFM and GFM models are shown in Figure 3. In the LFM model (*k*=0.6), when α was changed from 1.0 to 1.7 (*t*=3.0 s, indicated by the arrow), the *CL* decreased from 363 ms to the control value of 324.9 ms (Figure 3A), indicating the importance of the effects of acid-base concentration. When α was increased to 3.5, we could recover pacing function in cells with oscillation death (which was induced by increasing [ACh] to $5.0×10^{-8}$ mol L^{-1}) to the control state. In the GFM model (*k*=1.4), when α was changed from 1.0 to 0.2, the *CL* increased from 293.4 ms to the control value (Figure 3B).

2.3 Adjusting the temperature

Recent research found that it may be possible to change the heart rate by direct thermoregulatory effects on sinus node cells [23]. In patients with chronic heart failure, a 41°C

water bath for 10 min or a 60°C sauna for 15 min can increase the heart rate by 20–25 beats per minute [22]. A 37°C water bath for 15 min was reported to increase cardiac output, which is associated with an increase in heart rate [24,25]. The depolarization rate of the SAN is mainly determined by I_f, I_k and $I_{Ca,T}$. I_f plays a major role in the SAN pacing rate, and this current was modeled as follows [26]:

$$I_f = \lambda \cdot [g_{f,Na} \cdot y \cdot (V - E_{Na}) + g_{f,K} \cdot y(V - E_K)]. \quad (6)$$

As the conductivity parameter λ of I_f increases with increasing temperature, we could change the pacing rate by adjusting the temperature. In our simulations, we selected λ as an adjustable parameter and fixed $[ACh]=1.5\times10^{-8}$ mol L^{-1}. The results are shown in Figure 4. If $\lambda=1.0$, in the LFM model ($k=0.4$), the *CL* is 673 ms, which can easily cause sinus arrest ($t<3.0$ s, Figure 4A), whereas in the GFM model ($k=2.0$), the *CL* is 266 ms, which can cause sinus tachycardia and atrial fibrillation ($t<3.0$ s, Figure 4B). To reverse these two abnormal pacemaker functions back to the control values, λ was increased to 1.4 in the LFM model and decreased to 0.6 in the or GFM model. The arrows in Figure 4A and B show when the temperature was changed (at $t=3.0$ s).

This study investigated pacing rate as a function of λ for different mutation parameters k and different external stimuli. Figure 5 shows a contour plot with the mutation parameter k on the horizontal axis. The brightness of the region
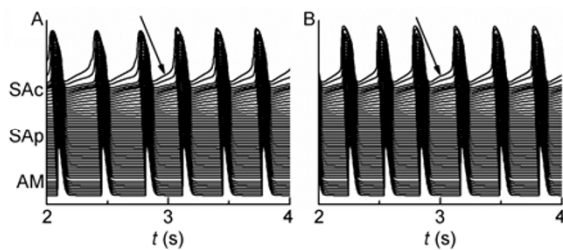

Figure 3 Effects of pH on SAN pacemaker function. $[ACh]=1.5\times10^{-8}$ mol L^{-1}. A, LFM model ($k=0.6$): at $t<3.0$ s, $\alpha=1.0$ and *CL*=363 ms; at $t>3.0$ s, $\alpha=1.7$ and *CL*= 324.9 ms. B, GFM model ($k=1.4$): at $t<3.0$ s, $\alpha=1.0$ and *CL*=293.4 ms; at $t>3.0$ s, $\alpha=0.2$ and *CL*=322.75 ms. The arrows show when α was changed.
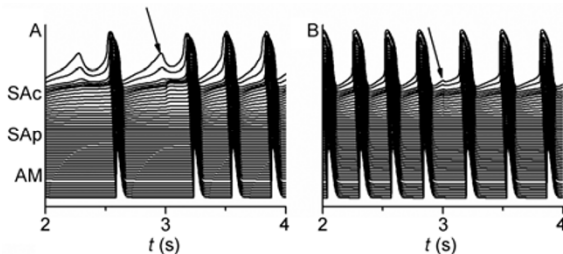

Figure 4 Effects of temperature on SAN pacemaker function. $[ACh]=1.5\times10^{-8}$ mol L^{-1}, $\lambda=1.0$. The arrows show when the temperature was changed (after 3 s). A, LFM model ($k=0.4$). When λ was changed from 1.0 to 1.4, the *CL* decreased from 673.3 ms to the control value of 329 ms. B, GFM model ($k=2.0$). When λ was changed from 1.0 to 0.6; *CL* increased from 266 ms to a control value of 329 ms.
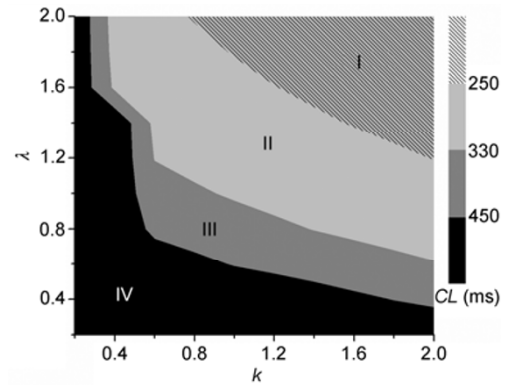

Figure 5 A contour plot of cardiac pacemaker function, divided into four regions according to the temperature parameter λ for different values of k. I, tachycardia area (*CL*<250 ms); II, normal rhythm area (250 ms<*CL*<330 ms); III, bradycardia area (330 ms<*CL*<450 ms); IV, oscillation death area (*CL*>450 ms).

represents the pacing rate. This figure shows that the dependence of pacemaker function on λ varies with k. The diagram can therefore be divided into four regions. In region I (where $\lambda>1.0$ and $k>0.8$), the SAN can pace spontaneously and continuously, because *CL*<250 ms, indicating tachycardia. In region III, the *CL* is 330–450 ms, indicating bradycardia. In region IV (*CL*>450 ms), pacing is completely suppressed; this is the oscillation death region where pacing cannot be recovered by external stimuli. In region II, the heart can beat normally without any external stimulus, unlike in regions I, III, and IV.

The results shown in Figure 5 suggest that pacemaker function can easily be recovered with appropriate external stimuli in all regions except for region IV. In regions I and III, which represent mutations that can cause abnormal pacemaker function or even sudden cardiac death, pacemaker function can be restored using one of the three above mentioned methods. For example, in region I ($\lambda>1.0$, $k>0.8$), the SAN can pace spontaneously and continuously, because *CL*<250 ms. As region I is mainly in the GFM region ($k>1.0$), the heart was usually tachycardic. When an external stimulus was applied in this area, i.e., when λ was changed from 1.0 to 0.6, the *CL* increased from 266 ms to the control value of 329 ms, and normal pacemaker function was recovered (Figure 4B). Normal pacemaker function was recovered using a similar method in region III.

In summary, we used an intact 2D anatomical rabbit heart model of the SAN and atrium with Na$^+$ channel LFMs and GFMs to quantitatively study the effects of three different external stimuli on pacemaker function. Our results show that GFM may cause tachycardia. In LFM, external stimulation may lead to cessation of pacing, which would cause sudden cardiac death. Our models show that abnormal oscillation or even a cessation of pacing is recoverable with the appropriated external stimuli.

The results of our simulation models may help in the development of clinical treatments. In this 2D anatomical mu-

tation model, parameters such as k, λ and acid-base concentration played very important roles in pacemaker function. Recovery of pacing was possible only under specific conditions (regions I, II, and III in Figure 5), and it was difficult to restart pacing under other conditions, especially in the LFM model with $k<0.3$ (region IV in Figure 5). Our findings may help to develop methods of treating cardiac arrhythmias, and to identify new methods for restarting pacing by regulating temperature or acid-base concentration.

1 Heribert S, Konig I R, Sekar K, et al. Large-scale association analysis identifies 13 new susceptibility loci for coronary artery disease. Nat Genet, 2011, 43: 333–338

2 Yang Y F, Zhu Y C, Li D Y, et al. Characterization of glucose-6-phosphate dehydrogenase deficiency and identification of a novel haplotype 487G>A/IVS5-612(G>C) in the Achang population of southwestern China. Sci China Ser C-Life Sci, 2007, 50: 479–485

3 Herfst L J, Book M B, Jongsma H J. Trafficking and functional expression of cardiac Na+ channels. J Mod Cell Cardiol, 2004, 36: 185–193

4 Shimizu W, Aiba T, Kamakura S. Mechanisms of disease: current understanding and future challenges in Brugada syndrome. Nat Clin Pract Cardiovasc Med, 2005, 2: 408–414

5 Juang J M, Huang S K. Brugada syndrome—an under-recognized electrical disease in patients with sudden cardiac death. Cardiology, 2004, 101: 157–169

6 Vatta M, Dumaine R, Varghese G, et al. Genetic and biophysical basis of sudden unexplained nocturnal death syndrome (SUNDS), a disease allelic to Brugada syndrome. Hum Mol Genet, 2002, 11: 337–345

7 Benson D W, Wang D W, Dyment M, et al. Congenital sick sinus syndrome caused by recessive mutations in the cardiac sodium channel gene (SCN5A). J Clin Invest, 2003, 112: 1019–1028

8 Dobrzynski H, Boyeet M R, Anderson R H. New insights into pacemaker activity: promoting understanding of sick sinus syndrome. Circulation, 2007, 115: 1921–1932

9 Schott J J, Alshinawi C, Kyndt F, et al. Cardiac conduction defects associated with mutations in SCN5A. Nat Genet, 1999, 23: 20–21

10 Chiang C E. Congenital and acquired long QT syndrome: current concepts and management. Cardiol Rev, 2004, 12: 222–234

11 Towbin J A, Vatta M. Molecular biology and the prolonged QT syndromes. Am J Med, 2001, 110: 385–398

12 Ackerman M J, Siu B L, Sturner W Q, et al. Postmortem molecular analysis of SCN5A defects in sudden infant death syndrome. JAMA, 2001, 286: 2264–2269

13 Plant L D, Bowers P N, Liu Q, et al. A common cardiac sodium channel variant associated with sudden infant death in African Americans, SCN5A S1103Y. J Clin Invest, 2006, 116: 430–435

14 Viswanathan P C, Balser J R. Inherited sodium channelopathies: a continuum of channel dysfunction. Trends Cardiovasc Med, 2004, 14: 28–35

15 Chen H S, Zhang J Q, Liu J Q. Selective effects of external noise on Ca^{2+} signal in mesoscopic scale biochemical cell systems. Biophys Chem, 2007, 125: 397–402

16 Zhang J Q, Qi F, Xin H W, Effects of noise on the off rate of Ca^{2+} binding proteins in a coupled biochemical cell system. Biophys Chem, 2001, 94: 201–207

17 Zhang H, Holden A V, Kodama I, et al. Mathematical models of action potentials in the periphery and center of the rabbit sinoatrial node. Am J Physiol Heart Circ Physiol, 2000, 279: 397–421

18 Zhang H, Zhao Y, Lei M, et al. Computational evaluation of the roles of Na+ current, I_{Na}, and cell death in cardiac pacemaking and driving. Am J Physiol Heart Circ Physiol, 2007, 292: 165–174

19 Timothy D B, Oleg V A, Shin I, et al. Mechanistic links between Na+ channel (SCN5A) mutations and impaired cardiac pacemaking in sick sinus syndrome. Circ Res, 2010, 107: 126–137

20 Honjo H, Boyett M R, Kodama I, et al. Correlation between electrical activity and the size of rabbit sino-atrial node cells. J Physiol, 1996, 496: 795–808

21 Wani B A, Khalil M Z, Al-Nozha M M, et al. Aborted sudden nocturnal cardiac death in a young man with structurally normal heart. Saudi Med J, 2005, 26: 323–325

22 Brian P D, Jonathan S. pH modification of human T-type calcium channel gating. Biophys J, 2000, 78: 1895–1905

23 Pakhcmov A G, Mathur S P, Doyle J, et al. Comparative effects of extremely high power microwave pulses and brief CW irradiation on pacemaker function in isolated frog heart slices. Bioelectromagnetics, 2000, 110: 351–360

24 Tei C, Horikiri Y, Park J C, et al. Acute hemodynamic improvement by thermal vasodilation in congestive heart failure. Circulation, 1995, 91: 2582–2590

25 Boone T, Westendorf T, Ayres P. Cardiovascular responses to a hot tub bath. J Alternat Compl Med, 1999, 5: 301–304

26 Rosenbaum T, Gordon S E. Quickening the pace: looking into the heart of HCN channels. Neuron, 2004, 42: 193–196